JOURNAL OF MATERIALS SCIENCE 10 (1975) 1481–1486

The esr behaviour of iron in gamma-irradiated Pyrex

G. BROWN
Physics Department, Royal Military College of Science, Shrivenham, Swindon, Wiltshire, UK

Iron, present as an impurity in commercial Pyrex tube, is examined by electron spin resonance (esr) as a function of γ dose. The population of Fe^{3+} initially decreases and then, at a well-defined dose, abruptly begins to increase. This behaviour is then correlated with lineshape changes to show that: (a) two distinct types of site must exist, occupied both by Fe^{2+} and by Fe^{3+}; (b) the site symmetry of the Fe^{3+} electron trap is different from that of the Fe^{2+} hole trap. Linewidth considerations show that a wider range of crystal fields exist in Pyrex than in the simpler types of glass.

1. Introduction

Since the first observations of electron spin resonance (esr) in a glass by Yasaitis and Smaller [1], research workers have been using esr to study the structures of different types of glass. The pioneering work of Sands [2] on paramagnetic impurities in glass laid the foundations for the esr study of glass structure by paramagnetic doping, a technique already well-established for the study of single crystals. If a glass is made from high-purity materials, no paramagnetic ions are present and no esr is observed. However, paramagnetic defects can be produced in the glass by suitable irradiation, the defect spectrum giving information on the environment of the defect.

The present work makes use of both impurity and defect spectra in commercially-available Pyrex tube. The spectrum of Fe^{3+} and its dependence on γ-irradiation will be discussed in this paper, while a treatment of the defect spectra is given separately [3].

2. Experimental

The samples used in all experiments were Pyrex tubes of 4 mm o.d. and 1 mm wall thickness. They were γ-irradiated by a ^{60}Co source at a dose rate of about 1.5 Mrad* h^{-1}, and the esr spectra were recorded at X-band on a JEOL spectrometer type PE-1X. First-derivative spectra were obtained in the usual way, the modulation frequency being 100 kHz. The microwave powers used in the experiments are given where necessary, and refer to the power incident on the cylindrical H_{011} cavity. Spin calibrations were performed using a standard $CuSO_4.5H_2O$ single crystal attached to the Pyrex tube being examined. All procedures were carried out at room temperature.

3. Results

3.1. The boron–oxygen hole centre (BOHC)

This defect centre, produced by γ-irradiation, is well-documented [1, 4-6], and is included here because its growth curve has a direct bearing on the behaviour of the iron resonance. The familiar "five-line-plus-a-shoulder" derivative curve of the BOHC is integrated twice as a function of dose to give the growth curve shown in Fig. 1. The growth is indicative of the two-stage process derived by Levy [7] and observed in Corning 7740 Pyrex by di Salvo *et al.* [8], with a saturation value in good agreement with the theory of Cropper [9].

3.2. The Fe^{3+} resonance

The principal paramagnetic impurities in Pyrex are iron [10] and vanadium [2, 11], easily recognised by their esr spectra. After γ-irradiation, any changes in the iron or vanadium spectra in the vicinity of $g = 2$ are completely swamped by the BOHC spectrum. However, the spectrum of Fe^{3+} is known to be smeared out over the range from $g = 1$ to $g = 10$ [10-12], with an isotropic resonance line centred on $g = 4.29$.

*The rad is a commonly-used unit of energy absorption. An absorbed dose of 1 megarad (Mrad) corresponds to an energy absorption input of 10 J.

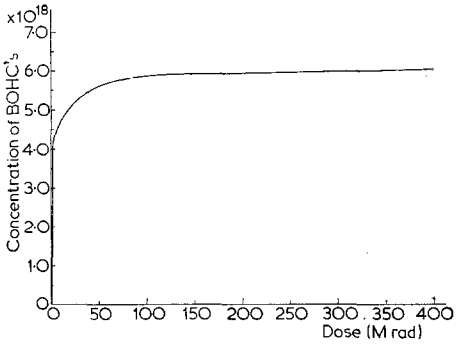

Figure 1 Growth curve of the BOHC. Microwave power 10 mW. Sample volume 1.66 cm³.

At X-band, this transition is about 0.2 T lower than the BOHC transitions and so can be studied for radiation effects with relative ease. Some typical lineshapes are shown in Fig. 2. These curves are representative of 400 spectra taken from 80 samples at different doses, and show that changes to lineshape and amplitude are produced. A "growth" curve for these results is given in Fig. 3. It is quite clear that two processes are active, one tending to reduce the number of Fe^{3+} centres, the other tending to increase it. The concentrations presented in Fig. 3 should be regarded with a little caution: they are obtained from curves such as are given in Fig. 2. Because these curves occupy only part of the total magnetic field gamut of the Fe^{3+} resonance, the corresponding concentrations represent only part of the total concentration.

4. Discussion

Before attempting to describe a model that will provide a qualitative explanation of the results, it is necessary to outline those traps which exist for holes and electrons.

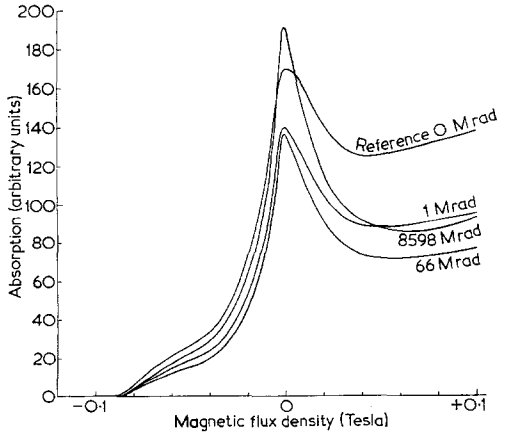

Figure 2 Lineshape of the Fe^{3+} resonance as a function of γ dose. Microwave power 10 mW. Magnetic flux density at centre = 0.158 T.

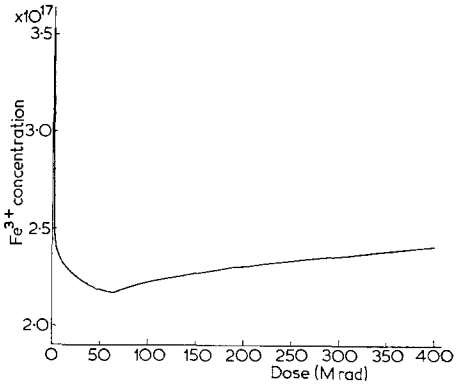

Figure 3 Variation of Fe^{3+} concentration with γ dose. Microwave power 10 mW. Sample volume 1.66 cm³.

4.1. Hole and electron traps

The dominant hole trap is an oxygen atom bridging two boron atoms [5]. On trapping a hole, it forms the boron–oxygen hole centre (BOHC). The second hole trap is Fe^{2+} [11, 13], which forms Fe^{3+} after trapping a hole.

The main electron trap is a void in the glass matrix [3, 14, 15]. The esr spectrum of an electron in such a trap in Pyrex, together with its growth curve in relation to this work, is described separately [3]. The other electron trap is the Fe^{3+} ion [11] which produces Fe^{2+} after trapping occurs. It is well known that these two valence states of iron co-exist in glasses [16-19] irrespective of the valence state present in the components of the melt.

All the signals observable optically and by esr following irradiation are attributable to the redistribution of electrons and holes. The effects reported here are all interconnected and are best understood by considering a "low-dose" and a "high-dose" region, these regions having a common diffuse boundary centred at about 100 Mrad.

4.2. The low-dose region

During irradiation, the ionized electrons and holes proceed to their respective traps. In the following analysis, recombination of the two carriers will be neglected; in other words, only the electrons and holes trapped (in preference to recombining) will be considered. Chemical analysis showed that iron was present at 0.027 wt% and thus it seems reasonable to assume that

the numbers of holes trapped by Fe^{2+} can be disregarded in comparison with those trapped by boron-associated oxygen, B_2O_3 being present at some 14 wt%. In this region, therefore, the only effective hole trap will form a BOHC. Electrons distribute themselves between the void traps and the Fe^{3+} ions. The latter, after trapping an electron, forms Fe^{2+} which cannot be observed by esr at room temperature [20]. However, a diminution of the existing Fe^{3+} resonance should occur as this valence conversion occurs. This reasoning is supported by the rapid increase of BOHC concentration observed experimentally in this region (Fig. 1) and by the rapid decrease observed in the Fe^{3+} concentration (Fig. 3).

4.3. The high-dose region

The above reasoning holds good up to a total dose of about 65 Mrad. At this point Fig. 1 shows that the dominant hole traps are 96% full, and the migrant holes begin to "see" the Fe^{2+} ions as their second type of trap. This mechanism, producing Fe^{3+}, should effect a change in the Fe^{3+} diminution established in the low-dose region. This is certainly the case, as Fig. 3 shows, and it is obvious that more Fe^{3+} is produced from hole capture by Fe^{2+} than is lost from electron capture by Fe^{3+} itself.

5. Interpretation

5.1. General behaviour

The curves of Fig. 3 can be linearized by adopting a logarithmic dose axis, as is done in Fig. 4, showing the marked reversal of direction at 65 Mrad. In Section 4.2 it was reasoned that, because of the very large ratio of boron-associated hole traps to Fe^{2+} hole traps, the numbers of holes trapped by Fe^{2+} could be disregarded in comparison with those trapped by the boron-associated centres. As Fig. 4 shows, the sharp change in the observed Fe^{3+} concentration at 65 Mrad would indicate that the Fe^{2+} centres are unable to trap holes until the boron-associated centres are almost saturated. From this premise, it can be seen that the diminution of the Fe^{3+} population should be representative of the process

$$Fe^{3+} + e \rightarrow Fe^{2+},$$

with no contribution from the reverse process

$$Fe^{2+} + h \rightarrow Fe^{3+}.$$

Because this is a pure reduction process (in the chemical sense of the word) and because the interconversion $Fe^{3+} \rightleftharpoons Fe^{2+}$ does not substantially alter the existing concentration of either component, an extrapolation of this reduction can be justified into the high-dose region. Combining the observed variation in the high-dose region with the extrapolated reduction process produces a pure oxidation behaviour. Fig. 4 illustrates the separation of the oxidation process from the observed growth behaviour.

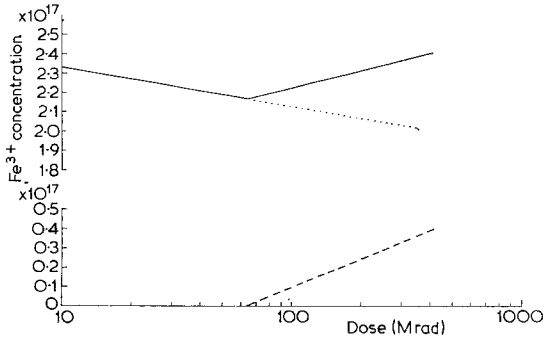

Figure 4 Variation of Fe^{3+} concentration with γ dose. Microwave power 10 mW. Sample volume 1.66 cm^3. Full line – observed variation. Dotted line – extrapolated reduction process. Broken line – derived oxidation process.

5.2. Site differences

An important distinction must be made between the Fe^{3+} sites involved in the reduction process and the Fe^{3+} sites created by hole trapping. The reduction process simply involves a diminution of the number of natural Fe^{3+} sites, but the oxidation process creates Fe^{3+} sites at natural Fe^{2+} sites. Work on natural Fe^{2+} and Fe^{3+} sites in glasses [10-13, 16-22] has provided much conflicting evidence. There is agreement that both valence states of iron can occupy tetrahedral and octahedral sites, i.e. either can occur as a network former or as a network modifier, the relative populations in the two sites being set by the total amount of iron and the type of glass. Mössbauer effect measurements are most commonly used in this type of investigation because both Fe^{2+} and Fe^{3+} give rise to Mössbauer spectra, in contrast to esr where only Fe^{3+} is visible. To the author's knowledge, the only work on borosilicate glass has been that of Taragin and Eisenstein [19] whose results show that both Fe^{2+} and Fe^{3+} are predominantly tetrahedrally co-ordinated, the Fe^{3+} almost certainly replacing Si^{4+} in SiO_4 tetrahedra. However, the width of the Fe^{2+} Mössbauer line is almost twice that

found in silicate and phosphate glasses, indicating that the Fe^{2+} ions experience a wide assortment of electric fields. Such a linewidth could be produced by Fe^{2+} ions in network modifier sites, the numbers of such ions being significantly greater than in the simpler glasses.

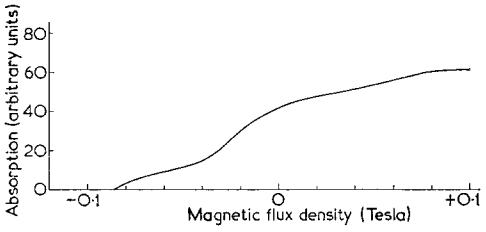

Figure 5 Spectrum of those Fe^{3+} ions which trap electrons to form Fe^{2+}. Magnetic flux density at centre = 0.158 T.

5.3. The significance of lineshape changes

The implications of site differences in the present work are important. In the unirradiated reference glass, the esr spectrum shown in Fig. 2 is that of the natural distribution of Fe^{3+} ions in 4- and 6-co-ordinated sites. It is clear that the lineshape, as well as the intensity, changes with dose. Taking the low-dose region alone, an algebraic subtraction of the 66 Mrad curve from the reference curve will reveal the spectrum of those Fe^{3+} centres which have been lost through electron capture. This spectrum is shown in Fig. 5. The following deductions can now be made.

(a) The electron trapping centres contribute principally to a "background" spectrum.

(b) There may be a small number of these centres which contribute to the isotropic ($g = 4.29$) resonance alone, thus causing the slight shoulder in the centre of Fig. 5.

(c) Alternatively to (b), there may be a small number of centres which generate the whole (background plus isotropic line) spectrum. These, too, would produce a small shoulder in the centre of the figure.

Of these deductions, (a) pertains to the great majority of the centres. Speculation over (b) and (c) will continue later.

In the high-dose region there is a different behaviour. By comparing the 8598 Mrad curve of Fig. 2 with the 66 Mrad curve, it can be seen that the $g = 4.29$ resonance has grown faster than the background resonance. The subtraction spectrum derived from these two curves is shown in Fig. 6 and it accentuates this fact. It has the two

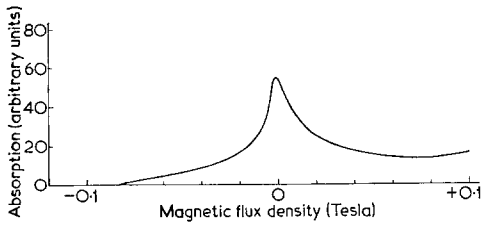

Figure 6 Spectrum of those Fe^{3+} ions produced from hole trapping by Fe^{2+}. Magnetic flux density at centre = 0.158 T.

characteristics of the reference spectrum of Fig. 2, the $g = 4.29$ peak superimposed upon a rising background. However, in Fig. 6 the ratio of the $g = 4.29$ amplitude to the maximum background amplitude is 3.3. In the reference glass, where the Fe^{3+} is in natural sites only, this ratio is 1.2, showing that the distribution of Fe^{3+} sites generated by hole capture at natural Fe^{2+} sites is markedly different from that of natural Fe^{3+} sites. The deductions from this behaviour are as follows.

(d) The Fe^{2+} hole-trapping centres are predominantly in sites whose symmetry generates the isotropic resonance from Fe^{3+}.

(e) The presence of a small background resonance could be due to hole-trapping by previously produced Fe^{2+} (i.e. $Fe^{3+} + e$).

(f) There could be small numbers of sites again generating the whole spectrum, as in (c) above.

5.4. Comparison with the literature

γ-irradiation of phosphate glasses is known to affect the Fe^{3+} resonance [18, 23], but because the results are quoted before and after one irradiation for three samples only, no parallels can be drawn with the present work.

The first tentative analysis of the iron resonance in glass by Castner *et al.* [10] ascribed the $g = 4.29$ resonance to Fe^{3+} ions in network-forming tetrahedral sites with rhombic distortion and the broad background to Fe^{3+} ions in network-modifying (octahedral) sites. Since then, this theory has been supported by Tucker [11], Hirayama *et al.* [24] and Bishay and Makar [18]. However, the work of Kurkjian and Sigety [22] provides evidence to the contrary, showing that rhombic symmetry at a tetrahedral and at an octahedral site would generate the isotropic resonance. Loveridge and Parke also support this view [12].

How, then, does the present work correlate

with the existing theories? Consider the following points.

(a) The $g = 4.29$ line in Pyrex is much broader than in the simpler glasses, indicating that there is a wider distribution of site symmetries here.

(b) If the complete spectrum had a single source, any diminution of the background intensity would be accompanied by a proportionate diminution of the isotropic line. As Fig. 5 shows, irradiation in the low-dose region removes the background spectrum alone. These two considerations lead inexorably to the conclusion that different sites are responsible for producing the two components of the spectrum.

Suppose site I generates the isotropic resonance and site II generates the background. Fe^{2+} and Fe^{3+} exist in both types of site, as Figs. 2, 5 and 6 indicate. The fact that the electron-trapping Fe^{3+} sites are type II shows that the electron affinity of Fe^{3+} in site II is very much greater than that of Fe^{3+} in site I. From the curve of Fig. 6 it can be seen that the hole affinity of Fe^{2+} in site I is greater than that of Fe^{2+} in site II, but not much greater. However, site II becomes a special case in the high-dose region because its natural Fe^{2+} population has been enhanced by a "rogue" Fe^{2+} population created in the low-dose region. It is quite probable that the hole affinities of the two populations are different, and it is reasonable to assume that the rogue population will have the greater hole affinity. Thus, the site II (background) component in Fig. 6 is most likely to be caused by reconversion of the rogue Fe^{2+} ions to their original Fe^{3+} state.

This model is not in contradiction with that of Kurkjian and Sigety [22]; their conclusion, that the isotropic and background components do not originate from sites of tetrahedral and octahedral co-ordination respectively, is not affected by the present results. There is some disparity between the model proposed here and that of Loveridge and Parke [12], but this is not altogether surprising because different glass systems are being compared. Their work on borate and silicate glasses led to the conclusion that "the entire background is associated with $g = 4.3$". This does not appear to be the case for Pyrex, where site I and site II have been invoked to characterize the isotropic and background components. As yet there is insufficient information to be specific about the symmetries of the two sites, but it must be stressed that they are obviously not separable into tetrahedral and octahedral sites.

6. Conclusions

Experiments on the γ-irradiation of commercial Pyrex tube have shown that the Fe^{3+} electron trap occupies a site of different symmetry from that of the Fe^{2+} hole trap, even though both valence states of iron occupy both types of site. The width of the isotropic $g = 4.29$ resonance indicates that a much larger distribution of crystal fields is to be found in Pyrex than in the simpler types of glass and, for this reason, the future identification of the symmetries of the two types of iron site may be a complicated process.

The detailed behaviour of the Fe^{3+} concentration with γ dose shows a reversal of direction at about 65 Mrad. This is shown to correlate with the growth of boron-oxygen hole centres (BOHC's). The observation and treatment of physically-trapped electrons in this context will be discussed separately [3].

References

1. E. L. YASAITIS and B. SMALLER, *Phys. Rev.* **92** (1953) 1068.
2. R. H. SANDS, *Phys. Rev.* **99** (1955) 1222.
3. G. BROWN, to be published.
4. S. LEE and P. J. BRAY, *J. Chem. Phys.* **39** (1963) 2863.
5. D. L. GRISCOM, P. C. TAYLOR, D. A. WARE and P. J. BRAY, *ibid* **48** (1968) 5158.
6. P. C. TAYLOR and D. L. GRISCOM, *ibid* **55** (1971) 3610.
7. P. W. LEVY, *J. Amer. Ceram. Soc.* **43** (1960) 389.
8. R. DI SALVO, D. M. ROY and L. N. MULAY, *ibid* **55** (1972) 536.
9. W. H. CROPPER, *ibid* **45** (1962) 293.
10. T. CASTNER JUN, G. S. NEWELL, W. C. HOLTON and C. P. SLICHTER, *J. Chem. Phys.* **32** (1960) 668.
11. R. F. TUCKER, "Advances in Glass Technology" (Plenum Press, New York, 1962).
12. D. LOVERIDGE and S. PARKE, *Phys. Chem. Glasses* **12** (1971) 19.
13. J. S. STROUD, J. W. H. SCHREURS and R. F. TUCKER, "Proceedings of the 7th International Glass Congress, Brussels 1965" (Gordon and Breach, New York, 1966).
14. A. EKSTROM and J. E. WILLARD, *J. Phys. Chem.* **72** (1968) 4599.
15. R. M. KEYSER, K. TSUJI and F. WILLIAMS, "The Radiation Chemistry of Macromolecules", Vol. 1 (Academic Press, New York, 1972).
16. A. A. BELYUSTIN, YU.M. OSTANEVICH, A. M. PISAREVSKII, S. B. TOMILOV, U. BAI-SHI and L. CHER, *Sov. Phys. Sol. Stat.* **7** (1965) 1163.
17. J. P. GOSSELIN, U. SHIMONY, L. GRODZINS and A. R. COOPER, *Phys. Chem. Glasses* **8** (1967) 56.
18. A. M. BISHAY and L. MAKAR, *J. Amer. Ceram. Soc.* **52** (1969) 605.

19. M. F. TARAGIN and J. C. EISENSTEIN, *J. Non-Cryst. Solids* **3** (1970) 311.
20. B. BLEANEY and K. W. H. STEVENS, *Rep. Progr. Phys.* **16** (1953) 108.
21. C. R. KURKJIAN and E. A. SIGETY, "Proceedings of the 7th International Glass Congress, Brussels 1965" (Gordon and Breach, New York, 1966).
22. *Idem, Phys. Chem. Glasses* **9** (1968) 73.
23. A. M. BISHAY, *J. Non-Cryst. Solids* **3** (1970) 54.
24. C. HIRAYAMA, J. G. CASTLE and M. KURIYAMA, *Phys. Chem. Glasses* **9** (1968) 109.

Received 7 February and accepted 18 March 1975.